Observation of the heat exchange during deformation using an infra-red camera

Joachim A. Koenen
Universität Ulm, Abt. Experimentelle Physik, Albert-Einstein-Allee 11, D-7900 Ulm, Germany
(Received 3 December 1991; accepted 13 March 1992)

The necking process during deformation of polycarbonate was observed with an infra-red (i.r.) camera. After calibration of the i.r. camera and determination of the emissivity of the sample, it is possible to transform the thermal image into a temperature image. Calculations, based on the heat conduction equation including heat sources and heat loss, yield a quantitative description of the measured temperature pattern and therefore the heat produced by the necking process. The method was checked by comparison with experiments done with a stretching calorimeter. The total balance of energy, heat and work could be measured as a function of the stretching rate. A transition from an increase of internal energy at low strain rates to an unchanged internal energy—all work is converted into heat—at high neck velocities is observed.

(Keywords: deformation; polycarbonate; polymeric glasses; necking; energy balance; infra-red camera)

INTRODUCTION

It is very common to do stretching experiments on and to measure the mechanical properties, e.g. force, strain and work, of materials[1–3]. But this is one side of the thermodynamic behaviour only. To get a more complete understanding of the processes that take place under deformation, one has to know the total exchange of energy, mechanical work *and* heat[4–6]. The Müller microstretching calorimeter[7] is one method to measure the thermomechanical properties of a material. Our method is another one. We observe the sample in a stretching device with an infra-red (i.r.) camera[8], measure the temperature changes and calculate the temperature pattern by using the equation of heat conduction including heat loss and heat sources. Comparison of the measured temperature image and calculation leads to the intensity of the heat sources and therefore to the heating up by deformation.

INFRA-RED CAMERA

For our experiments we use an Inframetrics 525 infra-red camera. The incoming i.r. beam passes through a germanium filter, which absorbs the visible and near-i.r. parts of the radiation. Two mirrors are used to scan the image vertically and horizontally. Zooming is possible by increasing the vibrational amplitude of the mirrors. A focus lens pictures the beam on the detector sitting in a liquid-nitrogen-cooled dewar[9]. It is a $Hg_x\,Cd_{1-x}Te$ semiconductor with a small band gap. A value $x \approx 0.3$ leads to a sensitivity in the spectral range 8–12 μm[10]. The i.r. camera converts the analogue signal of the detector using a six-bit analogue–digital converter and transforms it to a standard CCIR video signal (25 frames, 50 fields per second, 625 lines per frame). At the bottom of the video image a synthetically created grey level wedge is added. The technical data are collected in *Table 1*.

0032-3861/92/224732-05

EXPERIMENTAL SET-UP

The calibration, the determination of emissivity, reflectivity and transmittivity and the measurements during stretching are carried out with the following experimental set-up (*Figure 1*). The video signal from the i.r. camera is sent to an image splitter, where other signals from normal video sources, e.g. cameras, which observe the sample in the tensile tester (Zwick 1445), or displays, can be mixed with the i.r. signal to get a split video image. A clock and title generator adds information about the experiment and puts a clock into the video. This combined film is sent to a video recorder (Sony VO 7630 or VO 5630 Umatic). Further evaluation of the experiment is done with an image processing system (Imaging Technology PFG+) plugged into a personal computer.

First, after digitization, it does a grey level equalization using the wedge at the bottom of the image, to get rid of all influences of the transmission line. Transformation from thermal to temperature image, image analysis, image enhancements, temperature measurements and profiles are made with the frame grabber and the computer.

CALIBRATION

The whole system, starting with the i.r. camera, passing through the image splitter and clock generator, storage

Table 1 Technical data of the i.r. camera

Temperature range	−20 to 1300°C
Temperatue resolution	0.2 K
Spatial resolution	250 pixels per line 200 lines
Zooming range	4:1
Time resolution	50 fields, 25 frames per second
Detector	$Hg_xCd_{1-x}Te$ semiconductor
Output signal	CCIR norm video signal

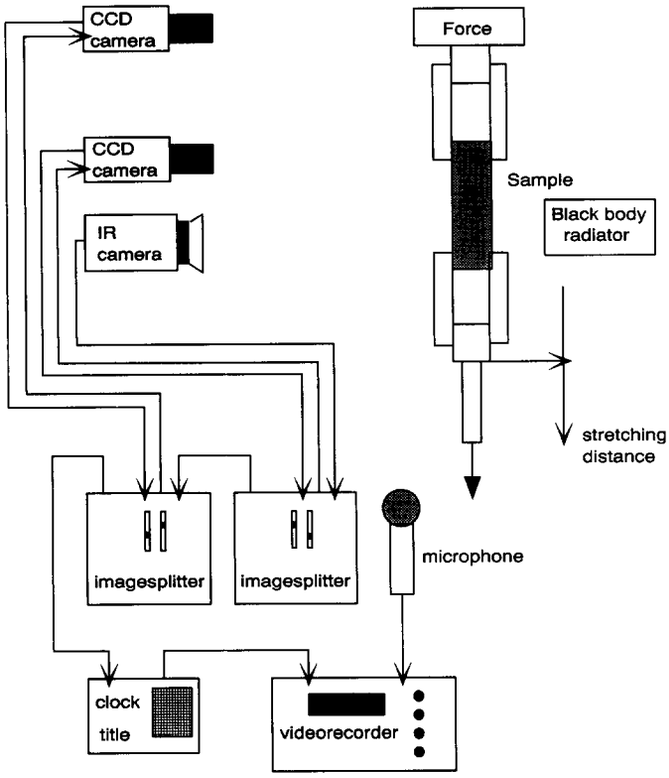

Figure 1 Experimental set-up for measurements with the i.r. camera during tensile tests and calibration. The i.r. camera observes the sample and the black-body radiator at the reference temperature. One video camera shoots at the line pattern on the sample to measure the local strains. The neck velocity is obtained by using the clock and the video film. The second video camera films the force display of the tensile tester. Comments and protocol are done with the microphone

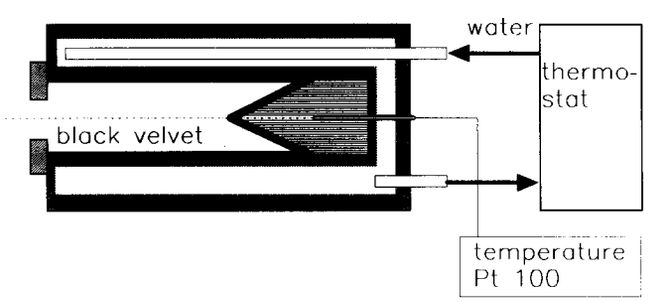

Figure 2 Sketch of the black-body radiator used for calibration and temperature reference

on the videotape and digitization of the film with the frame grabber, has to be calibrated before any temperature measurements are possible. To do this we observe two black-body radiators (*Figure 2*), one at a reference temperature T_{ref}, the other at the testing temperature T. The image processing system calculates the grey level difference between the two radiators. The results are seen in *Figure 3*. All grey level differences are related to a temperature of 20°C.

To understand these curves for the different range selections of the i.r. camera and to get a good interpolation between the measured points, let us calculate the signal of the camera.

A black-body with temperature T has the following spectral density[11]:

$$\rho(T, \lambda) = 2\pi hc^2\lambda^{-5}[\exp(hc/k_B T\lambda) - 1]^{-1} \quad (1)$$

with λ the wavelength, h Planck's constant, c the speed of light and k_B Boltzmann's constant.

The i.r. camera is sensitive at wavelengths between 8 and 12 μm. Assuming the sensitivity of the camera to be:

$$E(\lambda) = \left(\frac{\delta^2}{(\lambda - \lambda_{max})^2 + \delta^2}\right)^2 \quad (2)$$

with $\lambda_{max} = 10\ \mu$m and $\delta = 4\ \mu$m, the signal or the grey level in the thermal image respectively yields:

$$I(T) = G\int_0^\infty \mathrm{E}(\lambda)\rho(T, \lambda)\,\mathrm{d}\lambda + O \quad (3)$$

with the proportionality constant G and an offset O.

The full curves in *Figure 3* are calculated with equation (3) and give both an understanding of the calibration curves and a good interpolation function using two parameters only.

THERMAL IMAGE AND TEMPERATURE

The i.r. camera perceives objects because of their emission of electromagnetic radiation with wavelengths between 8 and 12 μm. An object with emissivity 1 radiates because of its temperature only. An object with an emissivity between 0 and 1 radiates partially due to its temperature and partially due to the reflected and transmitted radiation of its surroundings. Therefore, the thermal intensity seen by the camera can be written as:

$$I_{obj} = \varepsilon I_{bb}(T_{obj}) + \rho I_{bb}(T_{sur}) + \tau I_{bb}(T_{sur}) \quad (4)$$

with I_{bb} the intensity of a black-body with temperature T, T_{obj} and T_{sur} the temperatures of the object and its surroundings, ε the emissivity, ρ the reflectivity and τ the transmittivity.

Using:

$$\varepsilon + \rho + \tau = 1 \quad (5)$$

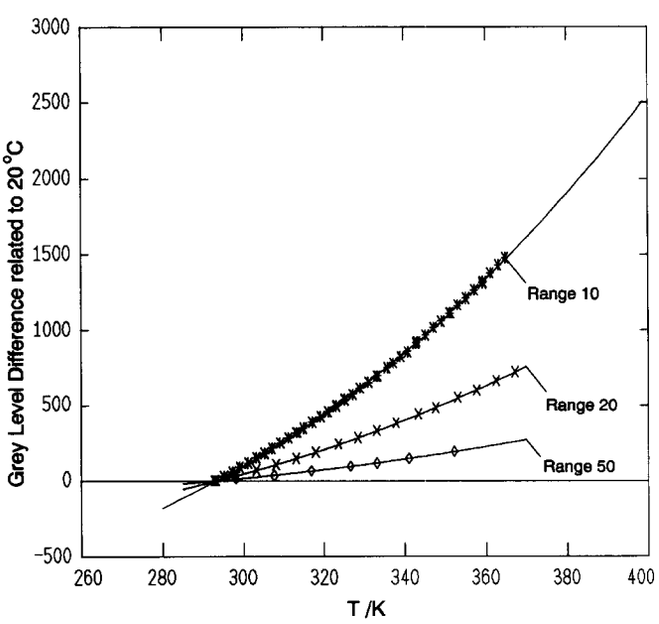

Figure 3 Calibration of the i.r. camera at different range selections. The full curves are calculations with equation (3). The grey level difference related to 20°C is plotted as a function of temperature

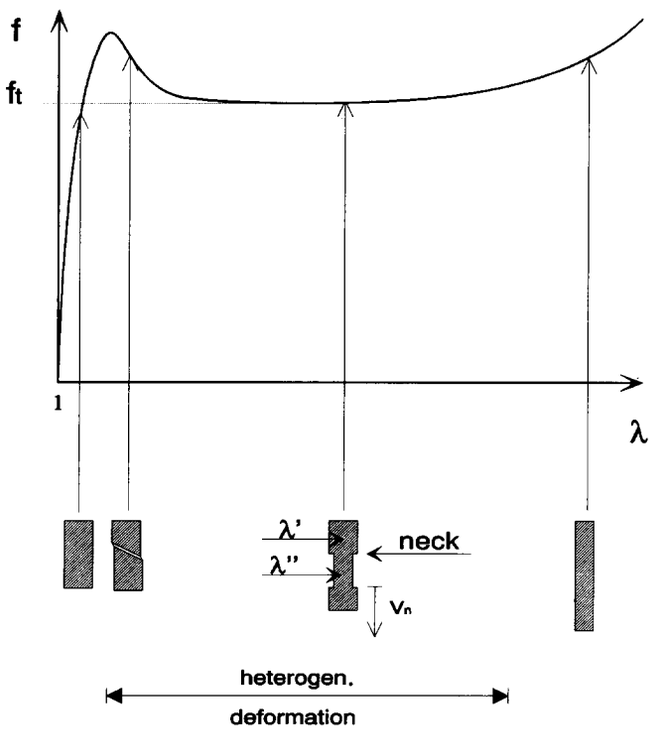

Figure 4 Schematic stress–strain curve of a polymeric glass showing a yield point and heterogeneous deformation (necking)

yields:

$$I_{obj} = \varepsilon I_{bb}(T_{obj}) + (1 - \varepsilon) I_{bb}(T_{sur}) \quad (6)$$

Since we are interested in the temperature of the object, rearrangement gives:

$$I_{bb}(T_{obj}) = (1/\varepsilon) I_{obj} + (1 - 1/\varepsilon) I_{bb}(T_{sur}) \quad (7)$$

Knowing the relation between I_{bb} and T from the calibration, the temperature of the object can be calculated.

Because of the difficulties of measuring the exact temperature of a free surface with a temperature difference to the surroundings, the emissivity ε was not measured directly. Instead we used the reflection and transmission of black-body radiation to get ρ and τ. The emissivity was calculated with equation (5). The transformation of the thermal image with equation (7) and the calibration results in a temperature image of the object and is done by the image processing system.

TEMPERATURE PATTERN OF A NECK

Many polymers and polymeric glasses, for example polycarbonate (PC), have a strange deformation behaviour. At the yield point, defined as the first relative maximum of the stress–strain curve, the deformation becomes heterogeneous[1,12–14]. A zone with a higher strain λ'' appears on the sample, while the rest has a lower strain λ'. On further stretching the boundary between the two zones with different strains λ' and λ'', which is called the neck, propagates with a constant velocity v_n at a constant nominal stress f_t over the sample. When the boundary has moved over the entire specimen, deformation becomes homogeneous again and stress and strain increase (*Figure 4*).

Because strain rate makes no sense when deformation becomes heterogeneous, the neck velocity v_n is used to characterize the speed of deformation. Besides this, strain rate is a function of machine speed and sample length, while the neck velocity is a function of machine speed only.

The transition from the lower deformed state λ' to the higher strain λ'' is accompanied by an exchange of mechanical work and heat[6]. The work per volume can be written:

$$w_t = f_t(\lambda'' - \lambda') \quad (8)$$

To determine the heat exchanged, we assume a heat source with a constant strength at the neck, where the deformation step $\lambda' \rightarrow \lambda''$ happens. This heat is produced homogeneously over the cross-section of the sample. It will disperse according to the law of heat conduction, will be lost at the surface due to heat transfer and will be transported with the material's deformation. Let us write the one-dimensional differential equation of heat conduction including heat sources and loss[15]:

$$\frac{\partial^2}{\partial x^2}\vartheta - \frac{1}{\kappa}\frac{\partial}{\partial t}\vartheta = -\frac{A}{K} + \frac{v}{\kappa}\vartheta \quad (9)$$

with t the time, ϑ the temperature difference to the surroundings, ρ_m the density, c the heat capacity, K the heat conductivity and $\kappa = K/(\rho_m c)$. On the right-hand side of equation (9) we have the source term A/K and the loss term with:

$$v = Hp/c\rho_m\omega \quad (10)$$

H being the heat transfer constant, p the perimeter and ω the cross-section. The necking process is responsible for the heat sources A and we assume an amount of heat q_t per volume being produced. Therefore we get:

$$A(x, t) = q_t \delta(x - v_n t) \quad (11)$$

where δ is the Dirac delta function. The last term in equation (9) describes the heat loss over the length of the sample, which is proportional to the temperature difference ϑ between sample and surroundings. This holds true for small temperature differences[15].

The solution of this differential equation for a neck propagating with velocity v_n on a sample with infinite length, passing the point $x = 0$ at time $t = 0$, is[16]:

$$\vartheta(x, t) = \frac{q_t v_n \sqrt{\kappa}}{2\sqrt{\pi}K} \int_{-\infty}^{\infty} dt'\, \Theta(t - t') \exp[-v(t - t')] \times \frac{1}{\sqrt{t - t'}} \exp[-(x - v_n t')^2/4\kappa(t - t')] \quad (12)$$

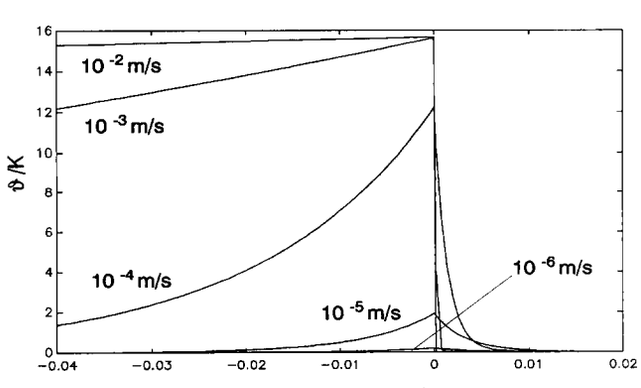

Figure 5 Theoretically calculated temperature profiles with equation (15) for different neck velocities with q_t = 19 MPa

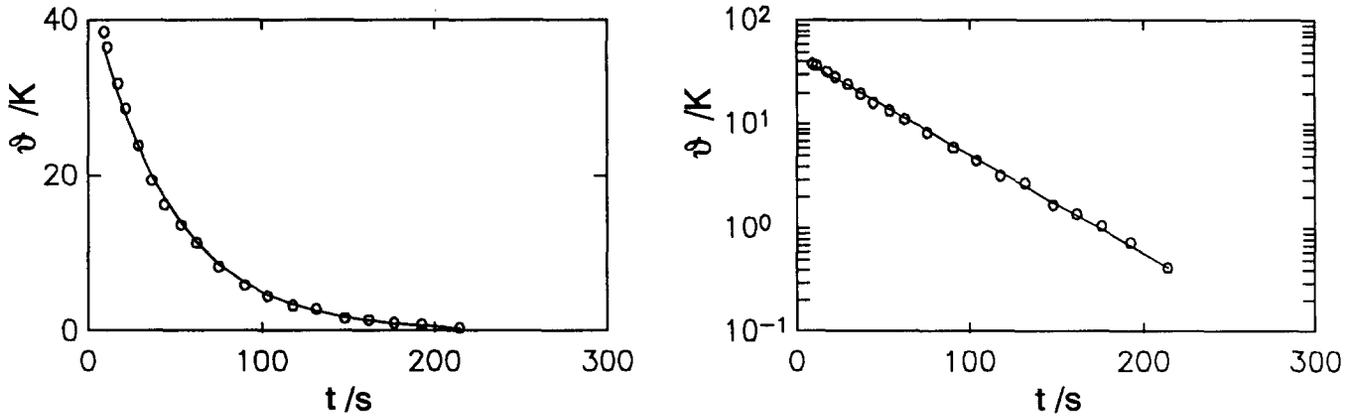

Figure 6 Change of temperature with time in a Newtonian cooling experiment. The full curve is calculated with equation (16) with $\vartheta_0 = 43.6$ K and $\nu = 0.021\ s^{-1}$. Samples are 1.06 mm thick and 10 mm broad

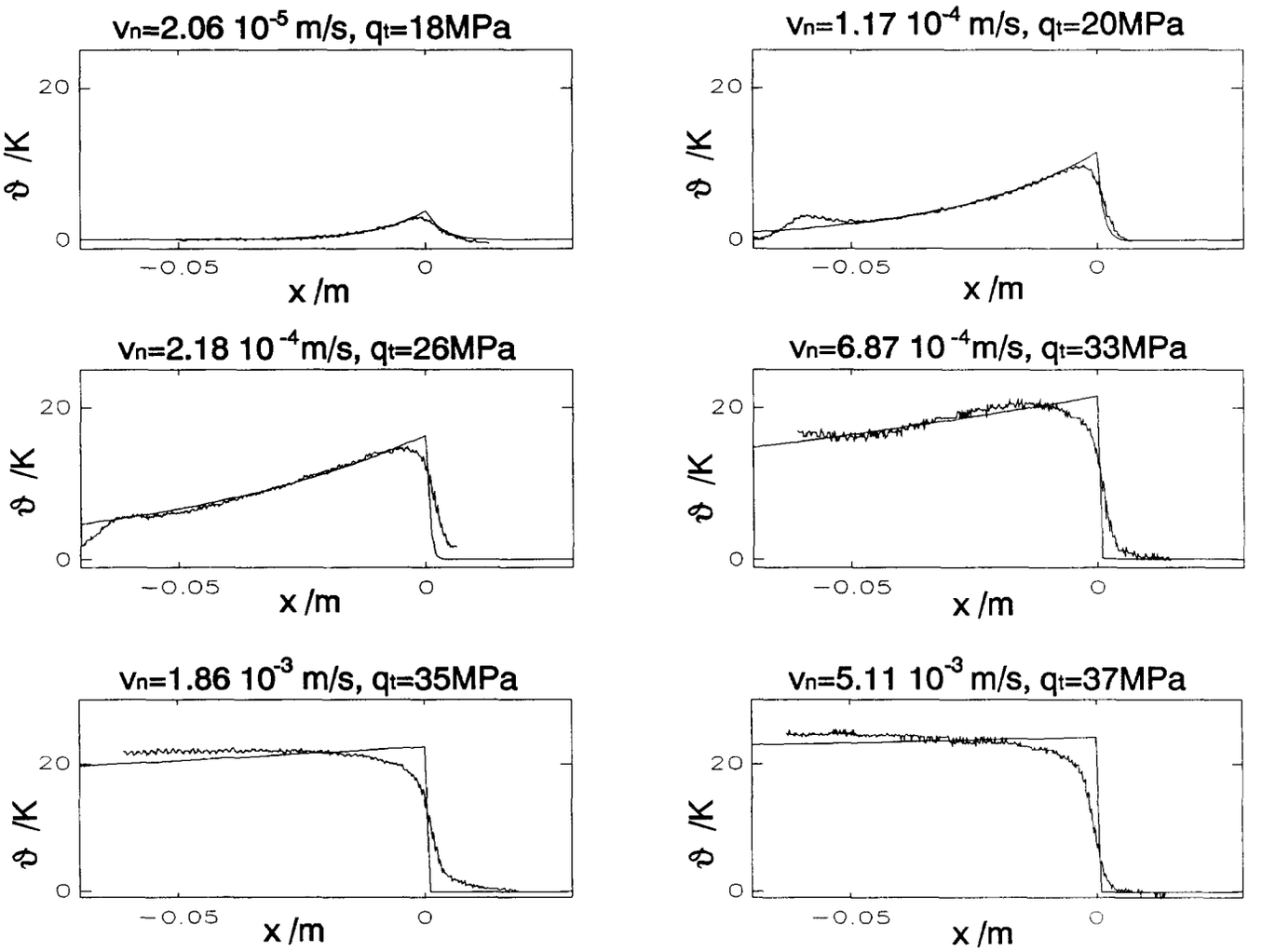

Figure 7 Measured and calculated temperature profiles of polycarbonate at room temperature with different stretching rates. Parameters collected in *Table 2*

If we change to the frame of reference co-moving with the neck:

$$x' = x - v_n t \tag{13}$$

we get a stationary solution, showing no time dependence:

$$\vartheta(x') = \frac{q_t v_n \sqrt{\kappa}}{2\sqrt{\pi} K} \int_{-\infty}^{\infty} d\tau\, \Theta(\tau) \exp(-v\tau) \times \frac{1}{\sqrt{\tau}} \exp[-(x' + v_n\tau)^2/4\kappa\tau] \tag{14}$$

The material behind the neck, which is already deformed from $\lambda' \to \lambda''$, transports the heat. This effect is a kind of convection. For our experimentally observed x'' we write therefore:

$$\begin{aligned} x'' &= x'\lambda''/\lambda' \quad \text{if } x' < 0 \\ x'' &= x' \quad \text{otherwise} \end{aligned} \tag{15}$$

Table 2 Parameters used for calculations

ε	0.94
ρ	0.06
τ	0.0
c	1.17 J K^{-1} g^{-1}
ρ_m	1.2 g cm^{-3}
K	0.21 W K^{-1} m^{-1}
H	13.86 W K^{-1} m^{-2}

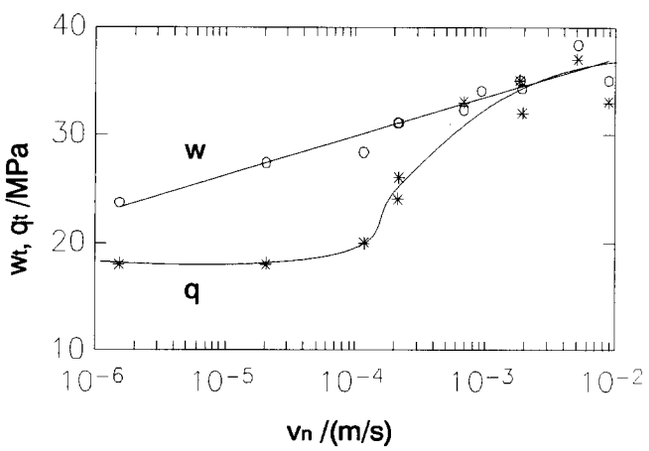

Figure 8 Work and heat of the transition $\lambda' \rightarrow \lambda''$ as a function of the neck velocity

In *Figure 5* we can see the solution of equations (14) and (15) for different neck velocities v_n and a constant q_t. At $v_n \approx 1.0 \times 10^{-6}$ m s^{-1} we have a nearly constant temperature over the length of the sample; at $v_n \approx 1.0 \times 10^{-2}$ m s^{-1} heat conduction and heat loss are too slow to have any effect. We have arrived at adiabatic deformation. Between these two values, we see a very characteristic temperature profile, from which it should be possible to evaluate the heat produced, q_t.

HEAT TRANSFER CONSTANT

In order to get the heat loss, which is described by the heat transfer constant v in equation (9), we perform a Newtonian cooling experiment. A sample with the same size as we use for the stretching experiments will be heated up to a temperature 10–40 K above the temperature of the surroundings. Bringing it into contact with the surroundings and observing the change of temperature with time, we measure an exponential decrease of temperature:

$$\vartheta(t) = \vartheta_0 \exp(-vt) \qquad (16)$$

From such experiments with different ϑ_0 and different ratios of perimeter p to cross-section ω, we have evaluated v for PC in air at room temperature (*Figure 6*). Using $\rho_m = 1.2$ g cm^{-3} for the density and $c = 1.17$ J K^{-1} g^{-1} for the specific heat yields a heat transfer constant $H = 13.86$ W K^{-1} mm^{-2} (equation (10)).

RESULTS AND DISCUSSION

The measured temperature profiles parallel to the stretching direction at different neck velocities are shown in *Figure 7* (see also *Table 2*). We can see a transition from nearly isothermal to adiabatic deformation. The descriptions of the measured temperature profiles with equations (14) and (15) are also added to the picture.

To check the correctness of our method we compare the results at low neck velocities with values measured in a stretching calorimeter[6]. In both cases we get 18 MPa (= mJ mm^{-3}) heat per volume for the transition $\lambda' \rightarrow \lambda''$.

The plot in *Figure 8* shows the mechanical work w_t and the heat q_t as functions of the neck velocity. At the highest strain rates the entire mechanical work is transformed into heat. Because it is not reasonable to produce more heat than the total mechanical work—this may be possible only in processes like strain-induced crystallization or something like that, which are not observed in PC—we arrive at a second fixed point of the complete energy balance[8]. Therefore the method with the i.r. camera measures the *entire* heat produced.

At a neck velocity of about 2×10^{-4} m s^{-1} we see a strong increase of q_t from a constant value at lower v_n until it reaches the work w_t. This behaviour may be a relaxational effect or a cooperative process, transforming the entire work into heat at high stretching rates. Therefore at low neck velocities internal energy increases with the transition $\lambda' \rightarrow \lambda''$, while at the highest speeds it remains constant.

The method developed to measure the complete energy balance during tensile tests is an extension of the measurements in a stretching calorimeter and may be denoted as 'fast calorimetry'.

REFERENCES

1 Haward, R. N. 'The Physics of Glassy Polymers', Applied Science, London, 1973
2 Bauwens-Crowet, C., Bauwens, J.-C. and Homès, G. *J. Polym. Sci. (A-2)* 1969, **7**, 735
3 Theodorou, D. N. and Suter, U. W. *Macromolecules* 1986, **19**, 379
4 Adams, G. W. and Farris, R. J. *J. Polym. Sci., Polym. Phys. Edn.* 1988, **26**, 433
5 Kilian, H. G. *Colloid Polym. Sci.* 1982, **260**, 895
6 Koenen, J. A., Kilian, H. G. and Heise, B. *J. Polym. Sci. (B) Polym. Phys.* 1989, **27**, 1235
7 Müller, F. H. and Engelter, A. *Kolloid Z.* 1957, **152**, 15
8 Maher, J. W., Haward, R. N. and Hay, J. N. *J. Polym. Sci., Polym. Phys. Edn.* 1980, **18**, 2169
9 'Operations Manual Model 525', Inframetrics Inc., Bedford, MA, USA, 1982
10 Long, D. and Schmitt, J. L. in 'Semiconductors and Semimetals' (Eds. R. K. Willardson and A. C. Beer), Academic Press, New York, 1970, Vol. 5
11 Planck, M. *Ann. Physik* 1900, **4**, 553
12 Theocaris, P. S. and Hadjiiossiph, C. *Eng. Fracture Mech.* 1979, **12**, 241
13 Hutchinson, J. W. and Neale, K. W. *J. Mech. Phys. Solids* 1983, **31**, 405
14 Nimmer, R. P. and Miller, L. C. *J. Appl. Mech.* 1984, **51**, 759
15 Carslaw, H. S. and Jaeger, J. C. 'Conduction of Heat in Solids', Clarendon Press, Oxford, 1959
16 Koenen, J. A. Vollständige Energiebilanz bei heterogener Kaltverformung von polymeren Gläsern, PhD Thesis, Universität Ulm, 1991